Assessing the characteristics of extreme precipitation over northeast China using the multifractal detrended fluctuation analysis

Haibo Du,[1] Zhengfang Wu,[1] Shengwei Zong,[1] Xiangjun Meng,[1] and Lei Wang[1]

[1]   Extreme climate events have inflicted severe and adverse effects on human life, social economy, and natural ecosystems. In this study, the precipitation time series from a network of 90 weather stations in Northeast China (NEC) and for the period of 1961–2009 are used. An objective method, the multifractal detrended fluctuation analysis method, is applied to determine the thresholds of extreme events. Notable occurrence frequency and strong intensity of extreme precipitation (EP) mainly occur in Liaoning Province and the piedmont regions in Changbai Mountains and Xiao Hinggan Mountains. Generally, EP frequency shows a nonsignificant negative trend, whereas EP intensity has a weak and nonsignificant positive trend for the entire NEC in the period of 1961–2009. To assess EP severity, we propose an EP severity index (EPSI) combining both EP frequency and intensity, rather than separately analyze the EP frequency or intensity. Spatial gradients of EPSI are observed in northeast-southwest and northwest-southeast directions over NEC. The EPSI in northwestern and southeastern NEC are low (0.02–0.3), whereas high EPSI (0.34–0.83) occurs in the southwestern and northeastern portions of the region. Higher EPSI (0.4–0.83) occurs in southern Liaoning Province, which decreases along the southwest-northeast direction. The spatial patterns of EPSI are associated with the circulation over East Asia. Areas that have a short distance from sea and that locate in the windward slope of mountain will probably accompany high EP severity over NEC.

Citation: Du, H., Z. Wu, S. Zong, X. Meng, and L. Wang (2013), Assessing the characteristics of extreme precipitation over northeast China using the multifractal detrended fluctuation analysis, *J. Geophys. Res. Atmos.*, *118*, 6165–6174, doi:10.1002/jgrd.50487.

1.   Introduction

[2]   Extreme climate events bring potential severe and adverse effects on human life, social economy, and natural ecosystems [*Santos et al*., 2009; *Li et al*., 2010; *Lupikasza*, 2010; *Dong et al*., 2011; *Mavromatis*, 2012]. Extreme precipitation (EP) is a major natural hazard [*Santos et al*., 2007]. Changes in EP events over large spatial scales have been described [*Jones et al*., 2004; *Rajczak et al*., 2013], whereas the variations in specific regions are not conclusively studied [*Kunkel*, 2003; *Wang et al*., 2008] and hence deserve further investigations [*Romero et al*., 2011]. Intensity and frequency of EP events vary among regions and within the duration of years [*Klein Tank et al*., 2006; *Beguería et al*., 2009]. Thus, EP studies at the regional scale are particularly important [*Beguería et al*., 2010; *Lupikasza*, 2010].

[3]   However, spatial patterns of EP changes are complex and vary from region to region worldwide [*Wang et al*., 2008]. For instance, increasing EP trends are reported for the Yangtze River basin [*Su et al*., 2006], the United States [*Kunkel et al*., 1999; *Griffiths and Bradley*, 2007], Japan [*Iwashima and Yamamoto*, 1993], Southern Brazil [*Liebmann et al*., 2010b], Korea [*Jung et al*., 2011], and India [*Sen Roy and Balling*, 2004]. In contrast, decreasing EP trends are found in other areas, including Southeast Asia and parts of the central Pacific [*Manton et al*., 2001], northern and eastern New Zealand [*Salinger and Griffiths*, 2001], Poland [*Bielec*, 2001], UK during summertime [*Osborn et al*., 2000], and some places in India [*Sen Roy and Balling*, 2004]. Particularly, *Kharin and Zwiers* [2005] reported an inconsistent conclusion that EP increases almost everywhere. On the one hand, these differences can be caused by the complexity, variability, and inherent difficulties in detecting trends of EP events [*Frei and Schär*, 2010]. On the other hand, they can be attributed to differences in methodology and definition of thresholds used to determine EP among researchers, which can obviously lead to different conclusions [*Wang et al*., 2008; *Zolina et al*., 2009]. For example, an extreme index (γ), defined as the ratio of EP days to the total number of precipitation days, decreased by 5%–10% in Northeast China (NEC) during

---

[1]School of Geographical Science, Northeast Normal University, Changchun, China.

Corresponding author: Z. F. Wu, School of Geographical Science, Northeast Normal University, Renmin St., No. 5268, Changchun 130024, China. (wuzf@nenu.edu.cn)
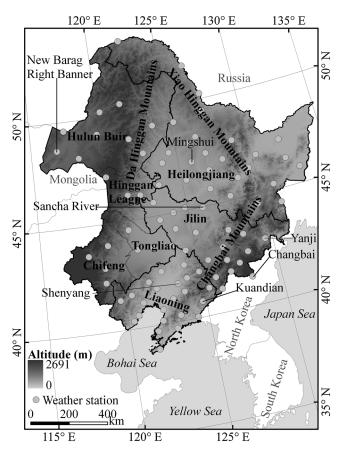
Figure 1. Study area and spatial distribution of the 90 weather stations tapped in this study, distributed in the area of 115°52′E–135°09′E, 38°72′N–53°55′N.

the period of 1960–2000 when the fixed threshold method (25 mm) was used. However, it increased by 5%–15% in the same area for the same period when the percentile method (at the 95th percentile) was employed [*Zhang et al.*, 2008]. Therefore, studies to better determine thresholds of extreme events are important and desirable [*Bonsal et al.*, 2001; *Liebmann et al.*, 2010a]. We have reviewed the recent literatures addressing this issue and generally grouped them into three methodology categories:

[4] 1. The fixed threshold method [*Karl et al.*, 1995; *Brunetti et al.*, 2004; *López-Moreno and Beniston*, 2009]. For example, EP over the Yangtze River basin is determined when daily precipitation is in excess of 50 mm [*Su et al.*, 2006].

[5] 2. The standard deviation method. For instance, *Schönwiese et al.* [2003] considered an EP day as a daily precipitation that exceeds a standard deviation of ± 2 or ± 3 times.

[6] 3. The percentile-based method, which is the most widely used method [*Liebmann et al.*, 2010a; *Lupikasza*, 2010; *Dong et al.*, 2011; *Jones et al.*, 2011; *Jung et al.*, 2011]. This method considers days with precipitation higher than percentiles of the 90th, 95th, 97.5th, or 99th as EP days or defines an extreme event at each station when a daily rainfall exceeds a certain percentage (e.g., 3%, 4%, or 5%) of its seasonal or annual mean [*Liebmann et al.*, 2010a].

[7] However, a commonly accepted method for regional extreme event analysis does not exist [*Wang et al.*, 2008;

Beguería et al., 2009]. The fixed thresholds are not suited for large regions where various climate types exist. As for the standard deviation method and percentile-based method, it remains debatable which standard deviation level or percentile level can better determine an extreme event. For example, the percentiles of the 90th [*Becker et al.*, 2008; *Lupikasza*, 2010], 95th [*Dong et al.*, 2011; *Jung et al.*, 2011], 97.5th [*Bell et al.*, 2004; *Sen Roy and Balling*, 2004], and 99th [*Christensen and Christensen*, 2004; *Zolina et al.*, 2004; *Rahimzadeh et al.*, 2009] have been used to investigate the same "extreme event" (EP event). These methods have subjective selectivity. Definition of extreme event using these methods will be affected by personal factors, which is the principal shortcoming of these methods. Hence, we need a more objective method.

[8] In terms of the severity of EP events, some researchers [e.g., *Meehl et al.*, 2005; *Zolina et al.*, 2005] have separately studied the frequency and intensity of EP events. However, the severity of EP events rests with both intensity and frequency [Intergovernmental Panel on Climate Change (*IPCC*), 2007]. Neither high-frequency EP events with low intensity nor low-frequency EP events with a high degree of intensity can accurately reflect the severity of EP events for an area in a long-time series. Obviously, EP events with high frequency and high degree of intensity can indeed be harmful for a given area. Therefore, we propose a new method to analyze the severity of EP events by combining both frequency and intensity of EP events. For this purpose, we will introduce an EP severity index (EPSI).

2. Data and Methods

2.1. Precipitation and Reanalysis Data

[9] The study area located at 115°52′E–135°09′E, 38°72′N–53°55′N consist of provinces of Heilongjiang, Jilin, and Liaoning, as well as cities of Chifeng, Tongliao, Hinggan League, and Hulun Buir in eastern Inner Mongolia (Figure 1). Daily precipitation data (rainfall amount) for 131 weather stations during the period of 1951–2009 from China Meteorological Data Sharing Service System (CMDSSS) (http://cdc.cma.gov.cn/index.jsp) are available [see also *Du et al.*, 2012]. In the raw data, quality control has been performed to eliminate the stations with inhomogeneities, discontinuities, or obvious outliers by CMDSSS. The observation apparatus and height of precipitation were changed before and after 1960 [*Liu and Li*, 2003]. Some sites have missing or inadequate data during the early operating period of 1951–1960. Therefore, we use the precipitation data in the period of 1961–2009 (remaining 90 sites). Eight sites of the 90 stations have 1 day data scarcity (accounting for 0.056‰), and one station has 2 day data scarcity (0.112‰). These missing data are replaced by 0. The replacements of few missing data would not influence the analysis for extremes. Finally, a set of 90 high-quality series are used and illustrated in Figure 1. We also use the data from the National Center for Environmental Prediction/National Center for Atmospheric Research (NCEP/NCAR) Reanalysis Project [*Kalnay et al.*, 1996]. The selected variables are the monthly mean sea level pressure and 6 hourly geopotential height in the period of 1961–2009 on a $2.5° \times 2.5°$ spatial grid (available from their website at http://www.esrl.noaa.gov/psd/).

2.2. Methods

2.2.1. Determination of the Extreme Event Thresholds

[10] Time-varying climatic data series exist in long-range memory correlation (power law correlation) [*Fraedrich*, 2002; *Feng et al.*, 2004], which can characterize the normal variations of time-varying climatic data [*Koscielny-Bunde et al.*, 1996]. Therefore, the time-varying features of climate data series, e.g., long-range correlation and scaling exponent [*Koscielny-Bunde et al.*, 1996], must be taken into consideration in determining the threshold of extreme climate event. *Kantelhardt et al.* [2002] proposed the multifractal detrended fluctuation analysis (MF-DFA) procedure to calculate the long-range correlation (DFA index) of time series data. About the details of this method, the readers are referred to the literature [*Kantelhardt et al.*, 2002].

[11] Extreme events are beyond the normal variation range of time series data, which cannot affect the DFA index of the entire (original) series. According to this point of view, the DFA index calculated by the MF-DFA method can determine the thresholds of extreme events, which was proven by *Yang et al.* [2008] using 10,000 data of the x component of the Lorenz equations for chaotic system. Supposing that y is precipitation series with length N, the definition process is as follows:

[12] 1. Step 1: Successive elimination of the data y_i $\{y_i, y_i \geq y_{\max} - d \times k\}$ from the maximum value ($y_{\max}$) of y to zero at an appropriate interval, where $k = 1, 2, 3, \ldots,$ INT($(y_{\max} - 0)$/d). Then we can successively obtain the new series z_m ($m = y_{\max} - d \times k$), where m is the removed data for each new series. The d value represents the resolution of this algorithm. The smaller the d value, the higher the resolution of this method, which will be unfortunately accompanied by larger calculated quantities, and vice versa. The resolution of the precipitation data in this study is 0.1 mm. It is not necessary to use the smallest interval (0.1 mm) to distinguish different EP events because of the rare occurrence of EP events and the obvious differences between EP amounts. However, some larger value (e.g., 10 mm) is not suitable. As such, to obtain accurate threshold and reduce the calculated quantities, the d value used in this paper is 1 mm.

[13] 2. Step 2: Calculation of the long-range correlation index (DFA index, D_m) for each new series z_m.

[14] 3. Step 3: As the m value changes, so does the corresponding D_m value. When the m value varies from the minimum to the maximum, the D_m value will converge to the DFA index of the original series. The m value is determined as the EP threshold for y when the change trends in D_m tend to be stable and converge to the DFA index of the original series.

2.2.2. Definition of EPSI

[15] The EP severity over a region during a particular period is determined by both EP frequency and intensity. The intensity of each EP event for each station is decided by the threshold and the value exceeding the threshold. The smaller the threshold and the larger the value exceeding the threshold, the stronger the intensity. For example, the thresholds for stations A and B are determined as 90 and 50 mm, respectively. The 1 day total precipitation amounts for these two sites are 120 and 80 mm, respectively, which can be easily determined as EP events. Then, the rainfall amounts exceeding the thresholds for them are both 30 mm. If the total precipitation amount is determined as EP intensity, the intensity of A is stronger than that of B. In contrast, the EP intensity of A is the same as that of B when the values (30 mm) exceeding the thresholds are determined as EP intensity. However, the threshold of one station represents local tolerance capacity. The larger the threshold, the stronger the tolerance, and vice versa. The excess part (30 mm) of B is comparatively more dangerous than that of A. Therefore, we define the EP intensity as the value of the precipitation amount exceeding the threshold divided by the corresponding threshold. The percentage of the ratio represents the EP intensity.

[16] Moreover, the total intensity for a particular period (e.g., 1 year) is not only decided by the intensity of each EP but also influenced by the occurrence frequency. Thus, the intensity used in this study is considered as the average EP intensity, which is equal to the value of the total intensity divided by the corresponding frequency in a certain time. Then, frequency and intensity (average intensity) become two independent factors influencing the EP severity. Spatial EPSI reveals spatial gradients of the occurrence of EP events during a certain period, whereas temporal EPSI represents the time-varying EP severity for a region. A higher value of the EPSI indicates more serious EP events. EPSI is determined by the following steps:

[17] 1. Step 1: For spatial EPSI, calculation of the total EP frequency (X_i, $i = 1, 2, 3, \ldots, n$) and average EP intensity (Y_i, $i = 1, 2, 3, \ldots, n$) during the entire research period for each station, where n is the number of the stations (90 sites in this study). For temporal EPSI, calculation of the annual merged EP frequency (X_i, $i = 1, 2, 3, \ldots, n$) and average EP intensity (Y_i, $i = 1, 2, 3, \ldots, n$) in the entire NEC for each year, where n represents the year (49 years in this study), i.e.,

$$Y = [(P - P_{\text{threshold}})/P_{\text{threshold}}] \times 100\% \tag{1}$$

where P is the daily precipitation amount greater than or equal to $P_{\text{threshold}}$ for each station, and $P_{\text{threshold}}$ is the corresponding threshold for that site.

[18] 2. Step 2: Standardization of the frequency and intensity, such that each has a dimensionless value between 0 and 1, i.e.,

$$x_i = (X_i - X_{\min})/(X_{\max} - X_{\min}) \quad (i = 1, 2, 3, \ldots, n) \tag{2}$$

and

$$y_i = (Y_i - Y_{\min})/(Y_{\max} - Y_{\min}) \quad (i = 1, 2, 3, \ldots, n) \tag{3}$$

where $X_{\min}$ and $X_{\max}$ represent the lowest and highest EP frequencies among the stations for spatial EPSI (or among the years for temporal EPSI), respectively. $Y_{\min}$ and $Y_{\max}$ are the weakest and strongest EP intensities among the stations for spatial EPSI (or among the years for temporal EPSI), respectively. Then, the values of x_i and y_i are the standardizations of frequency and intensity, respectively.

[19] 3. Step 3: Obtainment of the EPSI for each site or each year, i.e.,

$$\text{EPSI} = k_1 \times x_i + k_2 \times y_i (i = 1, 2, 3, \ldots, n) \tag{4}$$

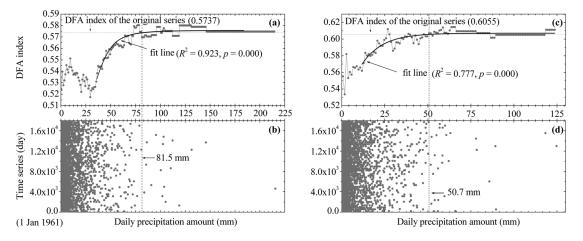where k_1 and k_2 are the weight coefficients of frequency and

Figure 2. Determination of EP threshold for Shenyang and Mingshui stations in 1961–2009, including analysis of the changes in (a and c) the DFA index and (b and d) the time-varying daily precipitation. R^2 is the coefficient of determination. The dashed line represents the thresholds, and the dotted line represents the DFA index of the original series.

intensity influencing EP severity, respectively, and $k_1 + k_2 = 1$. Intensity and frequency both play major roles in the severity of EP events [*IPCC*, 2007]. Therefore, k_1 and k_2 used in this paper are both 0.5. As such, the dimensionless value of EPSI is in the range of 0–1.

2.2.3. Mann-Kendall-Sneyers Test for Abrupt Detection

[20] The Mann-Kendall-Sneyers test, a sequential version of the Mann-Kendall rank statistics [*Mann*, 1945; *Kendall*, 1975] proposed by *Sneyers* [1990], is widely employed in analyzing environmental data, including precipitation and temperature [*Mavromatis and Stathis*, 2011], streamflow [*Liu and Zheng*, 2004], and water-quality data [*Donohue et al.*, 2001]. In this study, we use the test to detect the monotonic trend and abrupt change of EPSI for the entire NEC during the period of 1961–2009. In accordance with the EPSI method mentioned above, when we calculate the temporal EPSI for the entire NEC, the annual EP frequencies for the whole region are the mergence of annual frequencies of the 90 stations. The yearly EP intensities for the entire study area are the average yearly intensities of the 90 sites. We then compute the annual EPSI for the whole region during the period of 1961–2009 and can obtain a length of 50 EPSI series.

3. Results

3.1. Determination of EP Thresholds

[21] In this paper, the EP thresholds are determined by the MF-DFA method. To intuitively understand the process determining the EP thresholds, we show the time-varying daily precipitation amount and the changes in D_m (DFA index) for two sites [Shenyang station (123°27′E, 41°44′N) and Mingshui station (125°9′E, 47°17′N)] during the period of 1961–2009 in Figure 2. As shown in Figures 2a and 2c, the D_m values change with the m value (daily precipitation amount). When the m value varies from 0 to a certain value, the D_m value will begin to converge to the DFA index of the original series if the original series have extreme values. In this study, when the D_m values begin to be stable and equal to the DFA index of the original series, the m value is determined as threshold (Figures 2a and 2c). The EP thresholds for Shenyang

and Mingshui are determined to be 81.5 and 50.7 mm/d, respectively, where the D_m values begin to be stable and equal to the DFA index of the original series. The EP occurrences for these two sites are 17 days (Figure 2b) and 29 days (Figure 2d) in the period of 1961–2009, respectively.

3.2. Comparison Analysis of Various Methods for Determining EP Thresholds

[22] Determining the thresholds of extreme climate events is the most important target activity on the research about this type of event. Various methods will obtain obviously different thresholds. Figure 3 displays the EP thresholds determined by different methods and the corresponding occurrence frequency of EP for all the 90 stations over NEC during the period of 1961–2009. Different percentiles result in obvious differences (Figures 3a–3d). The lower the percentile, the smaller the threshold, and vice versa. The 99.8th, 99th, 97.5th, and 95th percentiles will obtain the average thresholds of 60.3, 31.6, 16.4, and 8.8 mm/d and the corresponding mean occurrence frequencies of 26.2, 145.5, 443.5, and 887.7 days, respectively, for all sites in NEC during the last five decades. It is very difficult to determine which percentile level is right or better. According to the rare occurrence of EP event, it is comprehensible that the average EP occurrence frequency obtained by the 99.8th percentile (0.5 day/yr for each site) may be more worthy of concern than that determined by the 95th percentile (18.1 days/yr for each site). However, there are other percentiles, such as the 99.9th, 99.7th, and 99.5th percentiles. Some decisions about which percentile level actually determines the "extreme events" still need to be made.

[23] Figure 3e shows the threshold determined as the value of 3 times standard deviation. Similar to the percentile-based method, there are also other standard deviation levels, such as 2, 4, or 3.3 times standard deviations. The common query on which standard deviation level should be determined as thresholds has to be addressed. With regard to the fixed threshold of 50 mm (Figure 3f), it is not suited for the entire study region where climate differs quite a lot from one area to another. For example, the mean annual
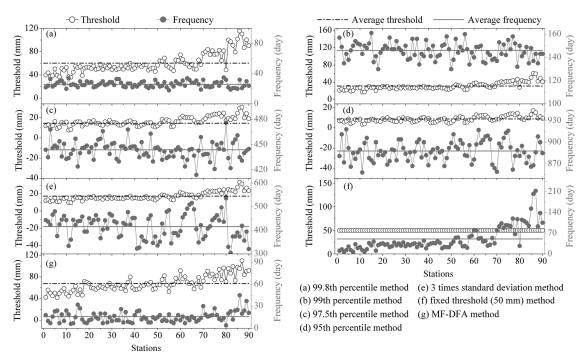
Figure 3. EP thresholds determined by different methods and the corresponding EP frequency for all 90 stations over NEC during the period of 1961–2009. The abscissa represents each site. (a–d) The signs denote the 99.8th, 99th, 97.5th, and 95th percentile methods, respectively. (e–g) The signs represent the 3 times standard deviation method, fixed threshold (50 mm) method, and MF-DFA method, respectively.

precipitation varies from 236.4 mm (New Barag Right Banner, 48.7°N, 116.8°E) to 1050.9 mm (Kuandian, 40.7°N, 124.8°E) in NEC. The threshold of 50 mm may be suited for New Barag Right Banner, but it is not suited for Kuandian, where 1 day 50 mm precipitation amount is normal. Figure 3g shows that the thresholds are determined by the MF-DFA method. According to this method, the average threshold and average frequency for each station are 67.9

mm/d (41.5–110.5 mm/d) and 15.6 days (4–45 days) in NEC, respectively. This result is similar to that obtained by the 99.8th percentile-based method (Figure 3a), which indicates that these EP events are actual rare events. Furthermore, the MF-DFA method does not have any other subjective selection, such as different percentile levels or various standard deviation levels. Determination of threshold by the MF-DFA method is based on the
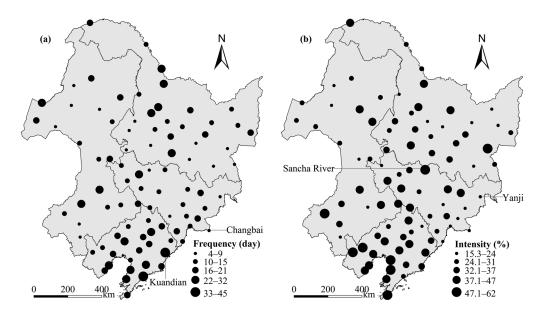

Figure 4. Spatial characteristics of (a) the EP frequencies and (b) the EP intensities over NEC during the period of 1961–2009. The frequency and intensity are the merged frequency and average intensity during the entire period of 1961–2009 for each station, respectively. The frequency and intensity units are days and %, respectively. The dots are scaled according to the amplitude of the value.
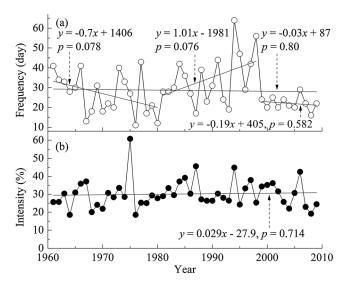
Figure 5. Change trends in (a) EP frequencies and (b) EP intensities over northeast China during the period of 1961–2009. The trend was calculated based on the linear regression. The 90 time series of frequencies and intensities are the annual total frequency and average intensity in the entire NEC for each year, respectively.

climatic time series data themselves, which reveals the "local tolerance capacity" of each site. The inherent local tolerance capacity should not be changed by different percentiles (percentile-based method), different standard deviations (standard deviation method), or various fixed values (fixed threshold method). Therefore, the MF-DFA method for determining EP threshold may be more objective, strict, and scientific than the others mentioned above. In this paper, we use the MF-DFA method to determine EP threshold.

3.3. Spatial Distributions of EP Frequency and Intensity

[24] Figure 4 shows the spatial distributions of the occurrence frequencies and average intensities of the EP event for all the 90 stations in the period of 1961–2009. The EP frequencies over NEC are obviously within the range of 4–45 days in the last five decades (Figure 4a). Notable occurrences of EP prevail in Liaoning Province and the piedmont region of the Xiao Hinggan Mountains, where the frequencies are in the range of 22–45 days. The highest EP frequencies are 45 days, which occurred in Kuandian (40.7°N, 124.8°E). The lowest EP frequencies (4 days) occurred in Changbai (41.4°N, 128.2°E) located at southern of Changbai Mountains. However, the stations with low EP frequencies do not have obvious distribution patterns. EP intensities are in the range of 15.3%–62% (Figure 4b). Similar to the distributions of EP frequencies, strong EP intensities of 47.1%–62% mostly occur in Liaoning Province and the piedmont region of Changbai Mountains. In contrast, the intensities in northwestern NEC are weaker. The weakest intensity of 15.3% occurred in Yanji (42.9°N, 129.5°E), whereas the strongest intensity of 62% occurred in Sancha River (45.0°N, 126.0°E).

3.4. Change Trends in EP Frequency and Intensity

[25] For investigating the change trends of EP frequencies and intensities over the entire NEC in the last 50 years, the 90 time series of frequencies and intensities are merged and averaged, respectively. Figure 5 shows the trend analysis of frequencies and intensities over the whole region. As shown in Figure 5a, the frequency has a weak negative trend of −0.3 day/10 years during the entire period. However, the trend is not significant at the 0.05 confidence level ($p = 0.80$). More complicatedly, there exist three periods with various change trends. The trend in EP frequency is negative during the period of 1961–1980, with a trend value of −7 days/10 years.
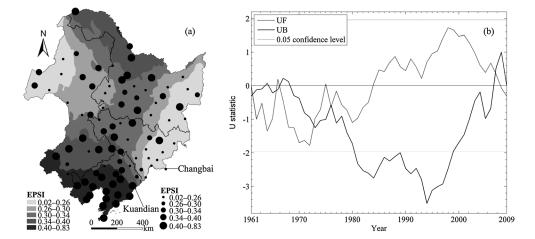

Figure 6. (a) Spatial patterns and (b) monotonic trend and abrupt change of EPSI over northeast China during the period of 1961–2009. The dots are scaled according to the amplitude of the indices. The larger the EPSI, the more serious the EP severity. The monotonic trend and abrupt change are detected using the Mann-Kendall-Sneyers (MKS) test at the 95% confidence level. *UF* (*UB*) is the forward statistic sequence estimated by the MKS test using an obverse (reverse) series of data. *UF* > 0 (*UF* < 0) indicates that an increasing (decreasing) trend exists somewhere in the time series. If an intersection of the forward and backward test statistic curves exists and occurs within the confidence interval, an abrupt change point is indicated.
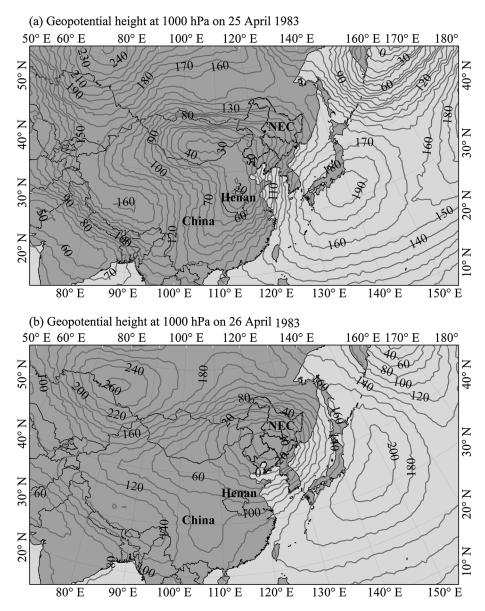
(a) Geopotential height at 1000 hPa on 25 April 1983

(b) Geopotential height at 1000 hPa on 26 April 1983

Figure 7. Average geopotential heights at 1000 hPa on (a) 25 April 1983 and (b) 26 April 1983, derived from global NCEP/NCAR reanalysis 6 hourly data. The unit is gpm.

In contrast, EP event has the increase trend of 10.1 days/10 years during 1981–1998. Then, the trend in EP frequency is again negative, with the value of -1.9 days/10 years. However, the trends of EP frequency in these three periods are not significant at the 0.05 confidence level. The highest occurrence EP frequency is 64 days in 1994, whereas the lowest occurrence EP frequency is in 1976, with a value of 11 days.

[26] Similar to the changes in the EP frequency, changes in the EP intensity also significantly affect society and the natural environment. With regard to the change trend in EP intensity (Figure 5b), it is distinct from that in EP frequency. EP intensity shows a nonsignificant linear change trend, with a very weak increase of 0.29%/10 years and a p value of 0.714 (at the 0.05 confidence level). There does not exist an obvious increase or decrease trend stage during the entire period. Instead, the intensity fluctuates around the average value. The strongest intensity of 60.8% occurred in 1975, whereas the weakest intensity occurred in 1964, with the

value of 18.5%. All these changes and nonsignificant trends indicate the complication and variability of EP frequency and intensity.

3.5. Spatiotemporal Features of EP Severity

[27] Figure 6 shows the spatiotemporal variation features of the EP severity over NEC during the period of 1960–2009. The spatial interpolation of EPSI is derived using the Kriging technique [*Oliver*, 1990]. Obvious northeast-southwest (NE-SW) and northwest-southeast (NW-SE) variation gradients of EPSI are found (Figure 6a). The EPSI value in northwestern and southeastern NEC is smaller than that in the other areas, which indicates that the EP events in these places are not substantial. The weakest EPSI of 0.02 occurred in Changbai. In contrast, the most serious EP events occurred in Liaoning Province and Xiao Hinggan Mountains. The strongest EPSI (0.83) occurred in Kuandian. The EP events along the NE-SW direction are more substantial. Interestingly,
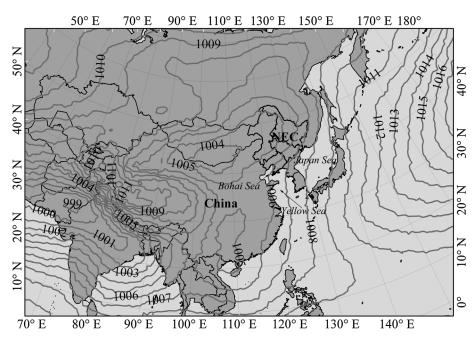
Figure 8. Summer (June–August) average sea level pressure during the period of 1961–2009, derived from global NCEP/NCAR reanalysis average monthly data. The unit is hPa.

they are distributed along the piedmont regions of the Changbai Mountains and Xiao Hinggan Mountains. Moreover, the severity trend negatively spreads along the southwest-northeast (SW-NE) direction from southwestern and northeastern NEC to central NEC.

[28] Figure 6b represents the monotonic trend and abrupt change of the regional annual time series detected using the Mann-Kendall-Sneyers test at the 95% confidence level for EPSI. The EPSI shows a clearly negative trend during the period of 1961–1984 and mainly positive from 1984 onward, whereas the trends are not statistically significant at the 95% confidence level. The significant abrupt change in EPSI primarily occurred in the period of 1965–1966, 1973, and 2006. Beginning from 1980, the decreasing trend became smaller and changed into a positive trend in 1984. However, the positive EPSI trend changed into a negative trend in 2009, which may be a happenstance.

4. Discussion and Conclusions

[29] The aims of our study are to investigate the spatiotemporal variations and trends in EP, as well as the EP severity, over NEC during the last five decades using the EPSI proposed in this study. We have done a comparative analysis of determining EP threshold using three main methods and the MF-DFA method. The MF-DFA method is selected as the most objective and scientific method among the four methods. The thresholds determined by the MF-DFA method for the entire NEC are similar to those determined by the 99.8th percentile method.

[30] One of the current main objectives in climate change studies is to determine whether trends in EP records are available [*Beguería et al.*, 2010]. *Pall et al.* [2007] suggested that EP increases proportionally with water vapor content (roughly 7.5%/°C warming). *O'Gorman and Schneider* [2009] noted that EP events in the midlatitudes increase more

slowly than the total moisture content. *Bartholy and Pongrácz* [2007] concluded that regional frequency and intensity of EP increase over the Carpathian Basin between 1976 and 2001. *Hamlet and Lettenmaier* [2007] found a significant increase in flood risk in many coastal areas. EP studies in China are far from satisfactory and have not provided definite information on how EP frequency and trend vary under global warming [*Zhang et al.*, 2008]. *Feng et al.* [2007] reported that decreasing trends in EP are mainly observed in northern China, whereas increasing trends are observed in the Yangtze River basin. A study of the Yangtze River basin showed that the number of days of EP (≥50 mm) increased considerably, but the change in intensity was insignificant [*Su et al.*, 2006]. Our study found that the EP frequencies are 4–45 days, and the intensities are in the range of 15.3%–62% over NEC during the last five decades. Both high-frequency and high-degree intensities are mainly distributed in Liaoning Province and the piedmont regions of the Changbai Mountains and Xiao Hinggan Mountains. Generally, EP frequency shows a negative trend, whereas EP intensity has a weak positive trend for the entire NEC in the period of 1961–2009. However, the trends are not significant at the 0.05 confidence level. We just analyzed the trends in EP frequency and intensity for the entire study area, rather than researched on the trends for each station, due to the nondeterminacy and the few or rare occurrences of EP event. To investigate the trends of EP frequency and intensity for each site, more recorded data are needed.

[31] Many researchers separately studied the EP frequency or intensity. However, EP severity in a region during a certain time is determined by both EP frequency and intensity; hence, considering both factors simultaneously can improve our understanding of evaluating the EP events. The study reveals obvious NE-SW and NW-SE spatial gradients in EPSI. The EPSI in northwestern and southeastern NEC is small, whereas the EPSI in southwestern and

northeastern NEC is large. The area with the most serious EPSI is in Liaoning Province, and the severity decreasingly spreads along the SW-NE direction to central NEC. The atmospheric circulation is one important factor causing an EP event. For example, Figure 7 shows the average geopotential heights at 1000 hPa on 25–26 April 1983. A high-intensity Yellow River cyclone occurred in nearby Henan Province on 25 April 1983 (Figure 7a) and moved into NCE on 26 April 1983 (Figure 7b), which resulted in many EP event occurrences on that day. Almost all EP events in April occurred on 26 April 1983 (9 out of 10 days) over NEC during the period of 1961–2009. NEC is located in the East Asian monsoon region. EP events mainly occur in summer. The rainy season in NEC begins with the summer monsoon prevailing in this region [*Ding*, 2004]. According to the summer mean sea level pressure in the period of 1961–2009 (Figure 8), the warm and humid maritime airstream spread from the Bohai Sea and Yellow Sea to central NEC along the piedmont regions of the Changbai Mountains. The Xiao Hinggan Mountains are affected by the maritime airstream spread from the Japan Sea. The warm and humid airstream can result in plenty of rainfalls when it spreads toward high latitude or altitude. EP severity in these places is more substantial than that in other areas over NEC due to the terrain and the East Asian summer monsoon factors. These results indicate that areas with a short distance from sea and located in the windward slope of mountain will probably accompany high EP severity in NEC. The relationship between circulation and the spatial patterns of EPSI discussed in this study will help to understand the dynamical features underlying the observed EP event severity.

[32] The monotonic trend of EPSI in the regional interannual time series shows nonsignificant negative and positive trends during the period of 1961–1984 and from 1984 onward, respectively. The abrupt change in EPSI mainly occurred in the period of 1965–1966, 1973, and 2006, which is different from the result of the abrupt change in the annual EP days, concentrated mostly in the period of 1978–1982 in NEC [*Zhang et al.*, 2008]. They just analyzed the changes in EP frequencies based on the 95th percentile method, rather than the variations in EP severity, which is the main reason for this difference. A rise in surface temperature will increase the EP frequency and intensity [*Trenberth et al.*, 2003; *Allan and Soden*, 2008; *Berg et al.*, 2009], and the return periods for EP events are shorter under enhanced greenhouse conditions [*McGuffie et al.*, 1999]. Therefore, the variation of EPSI may be due to human-induced regional warming, such as increased population, fast development of modern industries, utilization of fossil fuel, excessive cutting of forest, reclamation of grasslands, and overgrazing over northeast China [*Du et al.*, 2011].

[33] EPSI combining both EP frequency and intensity eliminates the influence of frequency on intensity. This method can objectively determine the EP severity for a region during a certain time. It is expected to be developed and used at any location.

References

Allan, R. P., and B. J. Soden (2008), Atmospheric warming and the amplification of precipitation extremes, *Science*, *321*(5895), 1481–1484, doi:10.1126/science.1160787.

Bartholy, J., and R. Pongrácz (2007), Regional analysis of extreme vtemperature and precipitation indices for the Carpathian Basin from 1946 to 2001, *Global Planet. Change*, *57*(1), 83–95, doi:10.1016/j.gloplacha.2006.11.002.

Becker, S., H. Hartmann, M. Coulibaly, Q. Zhang, and T. Jiang (2008), Quasi periodicities of extreme precipitation events in the Yangtze River Basin, China, *Theor. Appl. Climatol.*, *94*(3), 139–152, doi:10.1007/s00704-007-0357-6.

Beguería, S., S. M. Vicente-Serrano, J. I. López-Moreno, and J. M. García-Ruiz (2009), Annual and seasonal mapping of peak intensity, magnitude and duration of extreme precipitation events across a climatic gradient, Northeast Spain, *Int. J. Climatol.*, *29*(12), 1759–1779, doi:10.1002/joc.1808.

Beguería, S., M. Angulo-Martínez, S. M. Vicente-Serrano, J. I. López-Moreno, and A. El-Kenawy (2010), Assessing trends in extreme precipitation events intensity and magnitude using non-stationary peaks-over-threshold analysis: A case study in Northeast Spain from 1930 to 2006, *Int. J. Climatol.*, *31*(14), 2102–2114, doi:10.1002/joc.2218.

Bell, J. L., L. C. Sloan, and M. A. Snyder (2004), Regional changes in extreme climatic events: A future climate scenario, *J. Clim.*, *17*(1), 81–87, doi:10.1175/1520-0442(2004)017<0081:RCIECE>2.0.CO;2.

Berg, P., J. Haerter, P. Thejll, C. Piani, S. Hagemann, and J. Christensen (2009), Seasonal characteristics of the relationship between daily precipitation intensity and surface temperature, *J. Geophys. Res.*, *114*, D18102, doi:10.1029/2009JD012008.

Bielec, Z. (2001), Long-term variability of thunderstorms and thunderstorm precipitation occurrence in Cracow, Poland, in the period 1896–1995, *Atmos. Res.*, *56*(1–4), 161–170, doi:10.1016/S0169-8095(00)00096-X.

Bonsal, B. R., X. Zhang, L. A. Vincent, and W. D. Hogg (2001), Characteristics of daily and extreme temperatures over Canada, *J. Clim.*, *14*(9), 1959–1976, doi:10.1175/1520-0442(2001)014<1959:CODAET>2.0.CO;2.

Brunetti, M., M. Maugeri, F. Monti, and T. Nanni (2004), Changes in daily precipitation frequency and distribution in Italy over the last 120 years, *J. Geophys. Res.*, *109*, D05102, doi:10.1029/2003JD004296.

Christensen, O., and J. Christensen (2004), Intensification of extreme European summer precipitation in a warmer climate, *Global Planet. Change*, *44*(1), 107–117, doi:10.1016/j.gloplacha.2004.06.013.

Ding, Y. H. (2004), Seasonal march of the East-Asian summer monsoon, in *East Asian Monsoon*, edited by C. P. Chang, pp. 30–53, World Sci., Singapore.

Dong, Q., X. Chen, and T. Chen (2011), Characteristics and changes of extreme precipitation in the Yellow-Huaihe and Yangtze-Huaihe Rivers Basins, China, *J. Clim.*, *24*(14), 3781–3795, doi:10.1175/2010JCLI3653.1.

Donohue, R., W. A. Davidson, N. E. Peters, S. Nelson, and B. Jakowyna (2001), Trends in total phosphorus and total nitrogen concentrations of tributaries to the Swan-Canning Estuary, 1987 to 1998, *Hydrol. Processes*, *15*(13), 2411–2434, doi:10.1002/hyp.300.

Du, H. B., Z. F. Wu, and M. Li (2011), Interdecadal changes of vegetation transition zones and their responses to climate in northeast China, *Theor. Appl. Climatol.*, *106*(1–2), 179–188, doi:10.1007/s00704-011-0432-x.

Du, H. B., Z. F. Wu, Y. H. Jin, S. W. Zong, and X. J. Meng (2012), Quantitative relationships between precipitation and temperature over northeast China, 1961–2010, *Theor. Appl. Climatol.*, doi:10.1007/s00704-012-0815-7.

Feng, G. L., W. J. Dong, and X. J. Jia (2004), Application of retrospective time integration scheme to the prediction of torrential rain, *Chin. Phys.*, *13*(3), 413–422, doi:10.1088/1009-1963/13/3/028.

Feng, S., S. Nadarajah, and Q. Hu (2007), Modeling annual extreme precipitation in China using the generalized extreme value distribution, *J. Meteorol. Soc. Jpn.*, *85*(5), 599–613, doi:10.2151/jmsj.85.599.

Fraedrich, K. (2002), Fickian diffusion and newtonian cooling: A concept for noise induced climate variability with long-term memory, *Stochastics Dyn.*, *2*(3), 403–412, doi:10.1142/S0219493702000492.

Frei, C., and C. Schär (2010), Detection probability of trends in rare events: Theory and application to heavy precipitation in the Alpine region, *J. Clim.*, *14*(7), 1568–1584, doi:10.1175/1520-0442(2001)014<1568:DPOTIR>2.0.CO;2.

Griffiths, M. L., and R. S. Bradley (2007), Variations of twentieth-century temperature and precipitation extreme indicators in the Northeast United States, *J. Clim.*, *20*(21), 5401–5417, doi:10.1175/2007JCLI1594.1.

Hamlet, A. F., and D. P. Lettenmaier (2007), Effects of 20th century warming and climate variability on flood risk in the Western US, *Water Resour. Res.*, *43*, W06427, doi:10.1029/2006WR005099.

Intergovernmental Panel on Climate Change (IPCC) (2007), *Climate Change 2007: Synthesis Report. Contribution of Working Groups I, II and III to the Fourth Assessment Report of the Intergovernmental Panel on Climate Change*, edited by Core Writing Team, R. K. Pachauri, and A. Reisinger, 104 pp., Geneva, Switzerland.

Iwashima, T., and R. Yamamoto (1993), A statistical analysis of the extreme events: Long-term trend of heavy daily precipitation, *J. Meteorol. Soc. Jpn.*, *71*(5), 637–640.

Jones C., D. E. Waliser, K. M. Lau, and W. Stern (2004), Global occurrences of extreme precipitation and the Madden-Julian Oscillation: Observations and predictability, *J. Clim.*, *17*(23), 4575–4589, doi:10.1175/3238.1.

Jones, C., J. Gottschalck, L. M. V. Carvalho, and W. Higgins (2011), Influence of the Madden-Julian Oscillation on forecasts of extreme precipitation in the contiguous United States, *Mon. Weather Rev.*, *139*(2), 332–350, doi:10.1175/2010MWR3512.1.

Jung, I. W., D. H. Bae, and G. Kim (2011), Recent trends of mean and extreme precipitation in Korea, *Int. J. Climatol.*, *31*(3), 359–370, doi:10.1002/joc.2068.

Kalnay, E., et al. (1996), The NCEP/NCAR 40-year reanalysis project, *Bull. Am. Meteorol. Soc.*, *77*(3), 437–471, doi:10.1175/1520-0477(1996)077<0437:TNYRP>2.0.CO;2.

Kantelhardt, J. W., S. A. Zschiegner, E. Koscielny-Bunde, S. Havlin, A. Bunde, and H. E. Stanley (2002), Multifractal detrended fluctuation analysis of nonstationary time series, *Physica A*, *316*(1–4), 87–114, doi:10.1016/S0378-4371(02)01383-3.

Karl, T. R., R. W. Knight, and N. Plummer (1995), Trends in high-frequency climate variability in the twentieth century, *Nature*, *377*, 217–220, doi:10.1038/377217a0.

Kendall, M. G. (1975), *Rank Correlation Measures*, 202 pp., Charles Griffin, London.

Kharin, V. V., and F. W. Zwiers (2005), Estimating extremes in transient climate change simulations, *J. Clim.*, *18*(8), 1156–1173, doi:10.1175/JCLI3320.1.

Klein Tank, A. M. G., T. C. Peterson, D. A. Quadir, S. Dorji, X. Zou, H. Tang, K. Santhosh, U. R. Joshi, A. K. Jaswal, and R. K. Kolli (2006), Changes in daily temperature and precipitation extremes in central and south Asia, *J. Geophys. Res.*, *111*, D16105, doi:10.1029/2005JD006316.

Koscielny-Bunde, E., A. Bunde, S. Havlin, and Y. Goldreich (1996), Analysis of daily temperature fluctuations, *Physica A*, *231*(4), 393–396, doi:10.1016/0378-4371(96)00187-2.

Kunkel, K. E. (2003), North American trends in extreme precipitation, *Nat. Hazards*, *29*(2), 291–305, doi:10.1023/A:1023694115864.

Kunkel, K. E., R. A. Pielke Jr., and S. A. Changnon (1999) Temporal fluctuations in weather and climate extremes that cause economic and human health impacts: A review, *Bull. Am. Meteorol. Soc.*, *80*(6), 1077–1098, doi:10.1175/1520-0477(1999)080<1077:TFIWAC>2.0.CO;2.

Li, Z., F. Zheng, W. Liu, and D. C. Flanagan (2010), Spatial distribution and temporal trends of extreme temperature and precipitation events on the loess plateau of China during 1961–2007, *Quat. Int.*, *226*(1–2), 92–100, doi:10.1016/j.quaint.2010.03.003.

Liebmann, B., C. Jones, and L. M. V. de Carvalho (2010a), Interannual variability of daily extreme precipitation events in the state of Sao Paulo, Brazil, *J. Clim.*, *14*(2), 208–218, doi:10.1175/1520-0442(2001)014<0208:IVODEP>2.0.CO;2.

Liebmann, B., C. S. Vera, L. M. V. Carvalho, I. A. Camilloni, M. P. Hoerling, D. Allured, V. R. Barros, J. Báez, and M. Bidegain (2010b), An observed trend in Central South American precipitation, *J. Clim.*, *17*(22), 4357–4367, doi:10.1175/3205.1.

Liu, C., and H. Zheng (2004), Changes in components of the hydrological cycle in the Yellow River Basin during the second half of the 20th century, *Hydrol. Processes*, *18*(12), 2337–2345, doi:10.1002/hyp.5534.

Liu, X. N., and Q. X. Li (2003), Research of the inhomogeneity test of climatological data series in China, *Acta Meteorol. Sin.*, *17*(4), 492–502.

López-Moreno, J. I., and M. Beniston (2009), Daily precipitation intensity projected for the 21st century: Seasonal changes over the Pyrenees, *Theor. Appl. Climatol.*, *95*(3–4), 375–384, doi:10.1007/s00704-008-0015-7.

Lupikasza, E. (2010), Spatial and temporal variability of extreme precipitation in Poland in the period 1951–2006, *Int. J. Climatol.*, *30*(7), 991–1007, doi:10.1002/joc.1950.

Mann, H. B. (1945), Nonparametric tests against trend, *J. Econom. Soc.*, *13*(3), 245–259, doi:10.2307/1907187.

Manton, M. J., P. M. Della–Marta, M. R. Haylock, K. J. Hennessy, N. Nicholls, L. E. Chambers, D. A. Collins, G. Daw, A. Finet, and D. Gunawan (2001), Trends in extreme daily rainfall and temperature in Southeast Asia and the South Pacific: 1961–1998, *Int. J. Climatol.*, *21*(3), 269–284, doi:10.1002/joc.610.

Mavromatis, T. (2012), Changes in exceptional hydrological and meteorological weekly event frequencies in Greece, *Clim. Change*, *110*(1–2), 249–267, doi:10.1007/s10584-011-0095-8.

Mavromatis, T., and D. Stathis (2011), Response of the water balance in Greece to temperature and precipitation trends, *Theor. Appl. Climatol.*, *104*(1–2), 13–24, doi:10.1007/s00704-010-0320-9.

McGuffie, K., A. Henderson-Sellers, N. Holbrook, Z. Kothavala, O. Balachova, and J. Hoekstra (1999), Assessing simulations of daily temperature and precipitation variability with global climate models for present and enhanced greenhouse climates, *Int. J. Climatol.*, *19*(1), 1–26, doi:10.1002/(SICI)1097-0088(199901)19:1<1::AID-JOC348>3.0.CO;2-T.

Meehl, G. A., J. M. Arblaster, and C. Tebaldi (2005), Understanding future patterns of increased precipitation intensity in climate model simulations, *Geophys. Res. Lett.*, *32*, L18719, doi:10.1029/2005GL023680.

O'Gorman, P. A., and T. Schneider (2009), The physical basis for increases in precipitation extremes in simulations of 21st-century climate change, *Proc. Natl. Acad. Sci. U. S. A.*, *106*(35), 14773–14777, doi:10.1073/pnas.0907610106.

Oliver, M. (1990), Kriging: A method of interpolation for geographical information systems, *Int. J. Geogr. Inf. Syst.*, *4*(3), 313–332, doi:10.1080/02693799008941549.

Osborn, T. J., M. Hulme, P. D. Jones, and T. A. Basnett (2000), Observed trends in the daily intensity of United Kingdom precipitation, *Int. J. Climatol.*, *20*(4), 347–364, doi:10.1002/(SICI)1097-0088(20000330)20:4<347::AID-JOC475>3.0.CO;2-C.

Pall, P., M. R. Allen, and D. A. Stone (2007), Testing the Clausius-Clapeyron constraint on changes in extreme precipitation under CO_2 warming, *Clim. Dyn.*, *28*(4), 351–363, doi:10.1007/s00382-006-0180-2.

Rahimzadeh, F., A. Asgari, and E. Fattahi (2009), Variability of extreme temperature and precipitation in Iran during recent decades, *Int. J. Climatol.*, *29*(3), 329–343, doi:10.1002/joc.1739.

Rajczak, J., P. Pall, and C. Schär (2013), Projections of extreme precipitation events in regional climate simulations for Europe and the Alpine Region, *J. Geophys. Res. Atmos.*, *118*, 3610–3626 doi:10.1002/jgrd.50297.

Romero, Y. L., J. Bessembinder, N. C. van de Giesen, and F. H. M. van de Ven (2011), A relation between extreme daily precipitation and extreme short term precipitation, *Clim. Change*, *106*(3), 393–405, doi:10.1007/s10584-010-9955-x.

Salinger, M. J., and G. M. Griffiths (2001), Trends in New Zealand daily temperature and rainfall extremes, *Int. J. Climatol.*, *21*(12), 1437–1452, doi:10.1002/joc.694.

Santos, J. A., J. Corte-Real, U. Ulbrich, and J. Palutikof (2007), European winter precipitation extremes and large-scale circulation: a coupled model and its scenarios, *Theor. Appl. Climatol.*, *87*(1), 85–102, doi:10.1007/s00704-005-0224-2.

Santos, J. A., C. Andrade, J. Corte-Real, and S. Leite (2009), The role of large-scale eddies in the occurrence of winter precipitation deficits in Portugal, *Int. J. Climatol.*, *29*(10), 1493–1507, doi:10.1002/joc.1818.

Schönwiese, C. D., J. Grieser, and S. Trömel (2003), Secular change of extreme monthly precipitation in Europe, *Theor. Appl. Climatol.*, *75*(3), 245–250, doi:10.1007/s00704-003-0728-6.

Sen Roy, S., and R. C. Balling Jr. (2004), Trends in extreme daily precipitation indices in India, *Int. J. Climatol.*, *24*(4), 457–466, doi:10.1002/joc.995.

Sneyers, R. (1990), *On the Statistical Analysis of Series of Observations*, 143 pp., World Meteorol. Soc, Geneva.

Su, B. D., T. Jiang, and W. B. Jin (2006), Recent trends in observed temperature and precipitation extremes in the Yangtze River Basin, China, *Theor. Appl. Climatol.*, *83*(1), 139–151, doi:10.1007/s00704-005-0139-y.

Trenberth, K. E., A. Dai, R. M. Rasmussen, and D. B. Parsons (2003), The changing character of precipitation, *Bull. Am. Meteorol. Soc.*, *84*(9), 1205–1218, doi:10.1175/BAMS-84-9-1205.

Wang, W., X. Chen, P. Shi, and P. Van Gelder (2008), Detecting changes in extreme precipitation and extreme streamflow in the Dongjiang River Basin in Southern China, *Hydrol. Earth Syst. Sci.*, *12*(1), 207–221, doi:10.5194/hess-12-207-2008.

Yang, P., W. Hou, and G. L. Feng (2008), Determining the threshold of extreme events with detrended fluctuation analysis [in Chinese with English abstract], *Acta Phys. Sin.*, *57*(8), 5333–5342.

Zhang, D. Q., G. L. Feng, and J. G. Hu (2008), Trend of extreme precipitation events over China in last 40 years, *Chin. Phys. B*, *17*(2), 736–742, doi:10.1088/1674-1056/17/2/062.

Zolina, O., A. Kapala, C. Simmer, and S. K. Gulev (2004), Analysis of extreme precipitation over Europe from different reanalyses: A comparative assessment, *Global Planet. Change*, *44*(1–4), 129–161, doi:10.1016/j.gloplacha.2004.06.009.

Zolina, O., C. Simmer, A. Kapala, and S. Gulev (2005), On the robustness of the estimates of centennial-scale variability in heavy precipitation from station data over Europe, *Geophys. Res. Lett.*, *32*, L14707, doi:10.1029/2005GL023231.

Zolina, O., C. Simmer, K. Belyaev, A. Kapala, and S. Gulev (2009), Improving estimates of heavy and extreme precipitation using daily records from European rain gauges, *J. Hydrometeorol.*, *10*(3), 701–716, doi:10.1175/2008JHM1055.1.